**Advances in Materials Research,** *Vol. 12, No. 3 (2023) 193-210*
https://doi.org/10.12989/amr.2023.12.3.193


# An exact solution of dynamic response of DNS with a medium viscoelastic layer by moving load

S.A.H. Hosseini*[1], O. Rahmani[2a], H. Hayati[3b] and M. Keshtkar[1c]

*[1]Buein Zahra Technical University, Buein Zahra, Qazvin, Iran*
*[2]Smart Structures and New Advanced Materials Laboratory, Department of Mechanical Engineering, University of Zanjan, Zanjan, Iran*
*[3]Faculty of Engineering and Information Technology, University of Technology Sydney, PO Box 123 Broadway, Ultimo, NSW 2007, Australia*

*(Received April 1, 2020, Revised March 26, 2023, Accepted March 27, 2023)*

**Abstract.** This paper aims to analyze the dynamic response of a double nanobeam system with a medium viscoelastic layer under a moving load. The governing equations are based on the Eringen nonlocal theory. A thin viscoelastic layer has coupled two nanobeams together. An exact solution is derived for each nanobeam, and the dynamic deflection is achieved. The effect of parameters such as nonlocal parameter, velocity of moving load, spring coefficient and the viscoelastic layer damping ratio was studied. The results showed that the effect of the nonlocal parameter is significantly important and the classical theories are not suitable for nano and microstructures.

**Keywords:** double nanobeam system; dynamic response; moving load; nonlocal elasticity; viscoelastic layer

## 1. Introduction

Recently nanostructures have gained the interest of researchers in numerous disciplines such as physics, chemistry and engineering due to their special properties that are resulted by their nanoscale dimension (Murmu and Adhikari 2010). They are in the forms of various nanoscale structures such as nanoparticles, nanowires and nanotubes, which show promising mechanical, chemical, electrical, optical and electronic properties (Dai *et al.* 1996, Kim and Lieber 1999). Nano-resonators, nano-actuators, nano-machines and nano-optomechanical systems are some of the commonest categories of nanostructures (Eichenfield *et al.* 2009, Frank *et al.* 2010).

According to the former studies, it can be observed that the material properties at the nano-scale are size dependent and successively the small length scale effect should be considered for a precise modeling of nano-structure (Pirmohammadi *et al.* 2014, Rahmani and Pedram 2014). To

*Corresponding author, Assistant Professor, E-mail: hosseini@bzte.ac.ir
[a]Ph.D., E-mail: omid.rahmani@znu.ac.ir
[b]Ph.D., E-mail: Hasti.Hayati@uts.edu.au
[c]Ph.D., E-mail: keshtkarmahdi@gmail.com


http://www.techno-press.org/?journal=amr&subpage=5 ISSN: 2234-0912 (Print), 2234-179X (Online)

overcome this limitation, several modifications of the classical continuum mechanics have been presented to admit the size effect in the nanostructures modeling. One broadly used size-dependent theory is the nonlocal elasticity theory (Pourseifi *et al.* 2015, Rahmani *et al.* 2015, Rahmani *et al.* 2015, Hayati *et al.* 2016, Hosseini and Rahmani 2016, Hosseini and Rahmani 2016, Rahmani *et al.* 2016, Al-Huniti and Alahmad 2017, Bensaid *et al.* 2017, Ebrahimi and Barati 2017, Ebrahimi *et al.* 2017, Kunbar *et al.* 2020). Following that, Hosseini *et al.* (2019) modeled the clamped-clamped and clamped-free single-walled carbon nanotubes subjected to the moving longitudinal force based on Eringen's nonlocal elasticity theory along with two different nonlocal parameters, namely nonlocal Rayleigh and nonlocal bishop theories. Khosravi *et al.* (2020) surveyed the time-dependent forced and free torsional vibrations of elastic single-walled carbon nanotube exposed to both exponential and harmonic external torques. Moreover, the effects of resonance behavior, elastic medium, some geometrical dimensions on the angular displacement was studied. Furthermore, Khosravi *et al.* (2020) illustrated the effect of the viscoelastic medium, torsional boundary spring, thickness on the forced torsional vibration and the size dependency on the natural responses, the results were compared with the Rayleigh-Ritz method. Hossein *et al.* (2020) carried out the nano scale torsional vibration behavior of the carbon nanotubes when it affected by a moving external torque and when the moving term removed from the structure, the effects of aspect ratio and mode number on the natural frequency and influences of the nonlocal parameter, excitation frequency along with some geometrical parameters were evaluated. Hosseini *et al.* (2020) worked on the dynamic behavior of the CNTs subjected to the linear and harmonic loadings to analyze the effect of the size-dependency, thickness and excitation frequency on the forced behavior. Also, the effect of the nonlocal parameter on the multiple number of the natural frequency were examined. Khosravi *et al.* (2020) utilized a triangular nanowire model to study on the natural responses of the modeled for clamped-clamped along with clamped-torsional spring boundary condition. The effects of the triangle edge and nonlocal parametric on the natural frequencies were examined. However, there exist some other works around different size-dependent theories (Bastanfar *et al.* 2019, Hamidi *et al.* 2019, Hamidi *et al.* 2020). Zhang *et al.* presented predictive models of the free vibration of Euler-Bernoulli beams subjected to a uniformly thermal environment using two-phase local/nonlocal mixture theory of strain- and stress-driven types (Zhang *et al.* 2022). Fernández-Sáez and Zaera studied in-plane free vibrations (axial and bending) of a Bernoulli–Euler nanobeam using the mixed local/nonlocal Eringen elasticity theory (Fernández-Sáez and Zaera 2017). Khaniki explored the flapwise vibrational behavior of rotating size-dependent beams by using Eringen's two-phase local/nonlocal model as a reliable theory (Khaniki 2018). Zhang and Qing studied both the well-posed strain-driven and stress-driven two-phase local/nonlocal integral models are used to study the size effect in the free vibration of

EulerBernoulli curved beams (Zhang and Qing 2022). In another study, Zhang and Qing explored the well-posedness of several common nonlocal models for higher-order refined shear deformation beams (Zhang and Qing 2022). Wang *et al.* studied on exact solutions for the static bending of Euler-Bernoulli beams using Eringen's two-phase local/nonlocal model. The results appeared that the integral model considered here had some advantages as compared with differential model. it was a consistent softening effect for bending, and there was no paradox when solving a cantilever beam problem (Wang *et al.* 2016). Romano *et al.* showed that existence of a solution of nonlocal beam elasto-static problems is an exception, the rule being non-existence for problems of applicative interest (Romano *et al.* 2017). Zhang and Qing investigated static bending behavior of functionally graded (FG) Timoshenko beams via both strain- and stress-driven two-phase local/nonlocal mixed integral models based on the bi-Helmholtz kernel (Zhang and Qing 2021).

Various investigations are conducted to study nano sandwich structures. Liew *et al.* studied the vibration behavior of Multi-Layered Graphene Sheets that were embedded in an elastic matrix using a continuum-based plate model. They derived an explicit formula to predict the natural frequencies and associated vibration modes of double-layered and triple-layered graphene sheets (2006). Murmu *et al.* developed an analytical method to determine the natural frequencies of the nonlocal double beam, which are used in nano-optomechanical system and sensor applications. It was revealed that the small scale effect has a significant effect on the transverse vibration of double nano-beam system (2010). In the other study, which was made by Murmu *et al.* the nonlocal vibration of double-nano-plate system, was considered. It was assumed that two nano-plates are bounded by an enclosing elastic medium. They established expression for bending vibration of double nano-plate system using the nonlocal elasticity and also introduced an analytical model to derive the natural frequencies of Nonlocal Double-Nano-plate System (2011). Pouresmaeeli *et al.* presented an analytical approach for free vibration analysis of all edges simply supported double orthotropic nano-plates. It was assumed that the two nano-plates are bonded by an internal elastic medium and surrounded by an external elastic foundation. They derived the governing equations according to the nonlocal theory (2012). Murmu *et al.* analyzed the vibration of coupled nano-beam system under initial compressive pre-stressed condition. Using the nonlocal theory expressions for bending-vibration of pre-stressed double nano-beam system is formulated. They also proposed an analytical method to obtain natural frequencies of the Nonlocal Double Nano-Beam System (Murmu and Adhikari 2012). Radic *et al.* (2014). analyzed buckling of double orthotropic nano-plates using the nonlocal elasticity theory. They assumed that two nano-plates are bounded by an internal elastic medium and are surrounded by external elastic foundation.

In the present paper, the dynamic response of a double nanobeam system with a medium viscoelastic layer, under a moving load is analyzed. The governing equations are based on the nonlocal elasticity theory. It is assumed that a viscoelastic layer has coupled two nanobeams together. An exact solution is presented for each nanobeam and the dynamic deflection is accomplished.

## 2. Nonlocal double-nanobeam system equation

According to nonlocal continuum theory of Eringen (1972), the stress field at a point $x$ in an elastic continuum not only depends on the strain field at the same point but also on strains at all other points of the body. The constitutive equation of the nonlocal stress tensor $\sigma_{ij}(x)$ that is related to the local stress tensor at point $x$, $t_{ij}(x)$ becomes

$$(1-(e_0a)^2\nabla^2)\sigma_{ij}(x)=t_{ij}(x) \tag{1}$$

where $\nabla^2$ is a Laplacian operator, $e_0$ is a material constant and $a$ is an internal characteristic length (e.g., lattice parameter) of the nanobeam structure. Therefore, the only nonzero nonlocal stress within the nanobeam structure is outlined as

$$\sigma_{xx}-(e_0a)^2\sigma_{xx,xx}=E\varepsilon_{xx} \tag{2}$$

where $E$ is the young's module of elasticity. According to the linear vibration with only small deformation, the dynamic equation of motion for the transversely vibration nanobeam can be

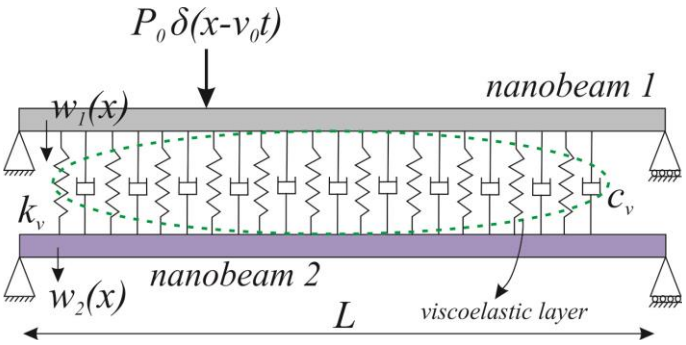


Fig. 1 The physical model of the nonlocal viscoelastic double-nanobeam system

obtained as

$$M_{,xx} + q = \rho A w_{,tt} \tag{3}$$

where $A$ is the cross-section of the nanobeam, $\rho$ is the density, $q$ is the distributed transverse load along $x$-axis and $M$ is the resultant bending moment which is defined by

$$M - (e_0 a)^2 M_{,xx} = -EI w_{,xx} \tag{4}$$

The explicit term of the nonlocal bending moment can be derived by substituting Eq. (4) into Eq. (3)

$$M = -EI w_{,xx} + (e_0 a)^2 \rho A w_{,tt} - (e_0 a)^2 q \tag{5}$$

The equation of motion for a nanobeam which is modeled as a Euler-Bernoulli beam and is in terms of the transverse deflection can be obtained by using Eqs. (3) and (5)

$$EI w_{,xxxx} - q + (e_0 a)^2 q_{,xx} + \rho A w_{,tt} - (e_0 a)^2 \rho A w_{,tt} = 0 \tag{6}$$

Fig. 1, shows a nonlocal double- nanobeam system bounded by a viscoelastic medium. The two nanobeams are assumed to be coupled by a viscoelastic medium. This medium is modeled by a vertical spring and vertical damper where, $k_v$ and $c_v$ are spring constant and damper coefficient, respectively. In this study, it is assumed that the two nanobeams have a same flexural rigidity $(EI)$ and mass per unit length $(\rho A)$.

$$(EI)_1 = (EI)_2 = EI, \quad (\rho A)_1 = (\rho A)_2 = \rho A \tag{7}$$

The transverse load for nanobeam 1 and 2 can be written as

$$\begin{aligned} q_1 &= k_v(w_2 - w_1) + c_v\left(w_{2,t} - w_{1,t}\right) + P \\ q_2 &= k_v(w_1 - w_2) + c_v\left(w_{1,t} - w_{2,t}\right) \end{aligned} \tag{8}$$

In the above equations, $w_1$ and $w_2$ represent transverse deflection for nanobeam 1 and 2, respectively. By substituting Eqs. (7) and (8) into Eq. (6), the equation of motion for nanobeam 1 and 2 expressed as:

Nanobeam 1

$$\begin{aligned} &EI w_{1,xxxx} + k_v(w_1 - w_2) + c_v\left(w_{1,t} - w_{2,t}\right) - P + (e_0 a)^2 k_v\left(w_{2,xx} - w_{1,xx}\right) \\ &+(e_0 a)^2 c_v\left(w_{2,txx} - w_{1,txx}\right) + (e_0 a)^2 P_{,xx} + \rho A w_{1,tt} - (e_0 a)^2 \rho A w_{1,ttxx} = 0 \end{aligned} \tag{9}$$

Nanobeam 2

$$EIw_{2,xxxx} + k_v(w_2 - w_1) + c_v\left(w_{2,t} - w_{1,t}\right) - P + (e_0a)^2k_v\left(w_{1,xx} - w_{2,xx}\right)$$
$$+(e_0a)^2c_v\left(w_{1,txx} - w_{2,txx}\right) + (e_0a)^2P_{,xx} + \rho Aw_{2,tt} - (e_0a)^2\rho Aw_{2,ttxx} = 0 \quad (10)$$

It should be noted that $P$ parameter in Eq. (9) represents a moving load that moves in axial direction of the primary nanobeam with constant velocity $v_0$.

$$P = P_0\delta(x - v_0t) \quad (11)$$

where $P_0$ is the magnitude of the moving load and $\delta(\cdot)$ is the delta function. For the sake of simplicity in solving Eqs. (9) and (10), we introduce the change of variable.

$$w = w_1 + w_2 \quad (12)$$

So that

$$w_1 = w - w_2 \quad (13)$$

By adding Eq. (9) to Eq. (10) and using Eq. (12),

$$EIw_{,xxxx} + \rho Aw_{,tt} - \rho A(e_0a)^2w_{,ttxx} = P - (e_0a)^2P_{,xx} \quad (14)$$

Substituting Eq. (13) into Eq. (10) and employing Eq. (12) leads to

$$EIw_{2,xxxx} + 2k_vw_2 + 2c_vw(e_0a)^2{}_{v\,2,xx_v}(e_0a)^2{}_{2,txx}{}_{2,t}$$
$$(\rho A)w_{2,tt} - \rho A(e_0a)^2w_{2,ttxx} = k_vw - k_v(e_0a)^2w_{,xx} + c_vw_{,t} - c_v(e_0a)^2w_{,txx} \quad (15)$$

At this stage, differential equation should be decoupled. It is assumed that nanobeams are simply supported and at each ends, the nonlocal bending moment and deflection are assumed to be zero

$$w_1(0,t) = w_1(L,t) = w_2(0,t) = w_2(L,t) = 0$$
$$M_1(0,t) = M_1(L,t) = M_2(0,t) = M_2(L,t) = 0 \quad (16)$$

By applying Eq. (12) in Eq. (16) leads to

$$w(0,t) = w(L,t) = 0$$
$$M(0,t) = M(L,t) = 0 \quad (17)$$

## 3. Analytical solution

In order to solve Eqs. (14) and (15), $w$ (total deflection) must be derived by using the solution of differential Eq. (14). Then by substituting total deflection into right hand side of Eq. (15), the dynamic response of the secondary nanobeam will be obtained:

### *3.1 Solution of undamped differential equation*

Using the normal mode method, the solution of Eq. (14) is assumed to be a linear combination of the normal mode of the nanobeam as follows

$$w(x,t) = \sum_{n=1}^{\infty} W_n(x)\eta_n(t) \quad (18)$$

Where $\eta_n(t)$ are the generalized coordinate and $W_n(x)$ are the normal mode of the simply supported nanobeam, which can be defined as

$$W_n(x) = \sin(\frac{n\pi}{L}x) \tag{19}$$

Substituting Eq. (18) into Eq. (14) and multiplying by $W_j(x)$ and then integrating from *0* to $L$, results in

$$\eta_{n,tt}(t) + \omega_n^2\eta_n(t) = Q_n(t) \tag{20}$$

Where

$$\omega = \sqrt{\frac{EI\left(\frac{n\pi}{L}\right)^4}{\rho A\left(1+(e_0a)^2\left(\frac{n\pi}{L}\right)^2\right)}} \tag{21}$$

In Eq. (20), $Q_n(t)$ is the generalized force corresponding to the *n* th mode and is given by

$$Q_n(t) = \frac{1}{g_n}\int_0^L W_n(x)\,P_0\delta(x - v_0\,t)\,dx = \frac{P_0}{g_n}sin(\frac{n\pi}{L}v_0\,t) \tag{22}$$

Where

$$g_n = \int_0^L \rho A W_n^2(x)dx = \frac{\rho AL}{2} \tag{23}$$

In this study, the initial conditions are assumed to be zero

$$w_1(x,0) = w_2(x,0) = w_{1,t}(x,0) = w_{2,t}(x,0) = 0 \tag{24}$$

Substituting initial equation into Eq. (12) leads to

$$w(x,0) = w_{,t}(x,0) = 0 \tag{25}$$

Therefore, $\eta_n(t)$ can be expressed as

$$\eta_n(t) = \int_0^t Q_n(\tau)\,h(t-\tau)\,d\,\tau \tag{26}$$

With

$$h(t) = \frac{1}{\omega_n}\sin(\,\omega_n t) \tag{27}$$

Substituting Eq. (24) into Eq. (26) and considering Eq. (27), leads to

$$\eta_n(t) = \frac{2P_0}{\rho AL\omega_n}\int_0^t \sin(\,t-\tau)\sin\left(\frac{n\pi v_0}{L}\tau\right)d\tau \tag{28}$$

Thus, the solution of Eq. (14) is given by (19) and (28)

$$w(x,t) = \frac{2P_0}{\rho AL}\sum_{n=1}^{\infty}\frac{sin\left(\frac{n\pi}{L}x\right)}{\left(\frac{n\pi v_0}{L}\right)^2 - \omega_n^2}\left[\frac{\frac{n\pi}{L}v_0}{\omega_n}\sin(\,\omega_n\,t) - \sin(\frac{n\pi}{L}v_0\,t)\right] \tag{29}$$

### *3.2 Solution of damping differential equation*

Now $w_2(x,t)$ can be derived from Eq. (15) by substituting Eq. (29) into Eq. (15) yields

$$EIw_{2,xxxx} + 2k_v w_2 - 2c_v w_{2,t} - 2(e_0 a)^2\, k_v w_{2,xx} - 2(e_0 a)^2\, c_v w_{2,txx} + \rho A w_{2,tt} - \rho A (e_0 a)^2 w_{2,ttxx} = \frac{2P_0\left(1+(e_0 a)^2\left(\frac{n\pi}{L}\right)\right)}{\rho A L} \sum_{n=1}^{\infty} \sin\left(\frac{n\pi x}{L}\right) U_n(t) \tag{30}$$

where

$$U_n(t) = \frac{k_v\left[\frac{\frac{n\pi}{L}v_0}{\omega_n} sin(\omega_n t) - sin\left(\frac{n\pi}{L}v_0 t\right)\right] + c_v \frac{n\pi}{L} v_0 \left[cos(\omega_n t) - cos\left(\frac{n\pi}{L}v_0 t\right)\right]}{\left(\left(\frac{n\pi}{L}v_0\right)^2 - \omega_n^2\right)} \tag{31}$$

Once again modal analysis is employed to solve Eq. (30)

$$w_2 = \sum_{n=1}^{\infty} W_{2n}(x)\eta_{2n}(t) \tag{32}$$

where $W_{2n}$ is the *n* th normalized normal mode, $\eta_{2n}(t)$ is the *n* th generalized coordinate. $W_{2n}$ is expressed as

$$W_{2n}(x) = \sin\left(\frac{n\pi}{L}x\right) \tag{33}$$

Similarly, substituting Eq. (32) into Eq. (30) and multiplying both side of the Eq.(30) by $W_{2i}(x)$ and then integrating it from $x = 0$ to $L$ leads to,

$$\eta_{2n,tt}(t) + 2\Omega_n \xi_n \eta_{2n,t} + \Omega_n^2 \eta_{2n}(t) = Q_n^*(t) \tag{34}$$

where $\Omega_n$ and $\xi_n$ denote the undamped natural frequency and damping ratio, respectively and are defined as

$$\xi_n = \frac{c_v}{\rho A \Omega_n}, \qquad \Omega_n = \sqrt{\frac{EI\left(\frac{n\pi}{L}\right)^4 + 2k_v\left(1+(e_0 a)^2\left(\frac{n\pi}{L}\right)^2\right)}{\rho A\left(1+(e_0 a)^2\left(\frac{n\pi}{L}\right)^2\right)}} \tag{35}$$

Now, the generalized force related to the *n* th mode is obtained as

$$Q_n^*(t) = \frac{1}{g_n}\int_0^L W_{2n}(x)\,\frac{2P_0}{\rho A L}\sum_{n=1}^{\infty} \sin\left(\frac{n\pi}{L}x\right) U_n(t)dx \tag{36}$$

Substituting Eq. (33) into Eq. (36) and using orthogonality property

$$\int_0^{L\int_{ij}} W_i(x) W_j(x) dx \tag{37}$$

where $\delta_{ij}$ is the Kronecker delta, leads to

$$Q_n^*(t) = \frac{2P_0}{\rho^2 A^2 L} U_n(t) \tag{38}$$

For zero initial condition, the generalized coordinate in the *n* th modes becomes as follows

$$\eta_{2n}(t) = \int_0^t \frac{1}{\Omega_{dn}} e^{-\xi_n \Omega_n (t-\tau)} \sin\left(\Omega_n(t-\tau)\right) Q_n^*(t-\tau)d\tau \tag{39}$$

where $\Omega_{dn}$ is the frequency of the damped vibration and is given by

$$\Omega_{dn} = \Omega_n\sqrt{1-\xi^2} \tag{40}$$

Substituting Eq. (38) into Eq. (39) and applying the integration leads to

$$\eta_{2n}(t)=\frac{2e^{-\xi\Omega_n t}P_0}{a_8}\begin{pmatrix}a_1\cos\left(\frac{n\pi v_0}{L}t\right)+a_2\sin\left(\frac{n\pi v_0}{L}t\right)+\\ v_0 n\pi(a_3\cos(\Omega_d t)+a_4(a_5\cos(\omega_n t)+a_6\sin(\omega_n t))+a_7\sin(\Omega_d t))\end{pmatrix}\quad(41)$$

where

$$\begin{aligned}
a_1&=-v_0 n\pi L^2 e^{\xi\Omega_n t}\omega_n\Omega_d\begin{pmatrix}\omega_n^4+2\omega_n^2\left(\xi^2{\Omega_n}^2-{\Omega_d}^2\right)\\+\left(\xi^2{\Omega_n}^2+{\Omega_d}^2\right)^2\end{pmatrix}\begin{pmatrix}{v_0}^2(n\pi)^2c_v+\\L^2\left(\xi\Omega_n(2k_v-c_v\xi\Omega_n)-c_v{\Omega_d}^2\right)\end{pmatrix}\\
a_2&=e^{\xi\Omega_n t}L^3\omega_n\Omega_d\begin{pmatrix}-{v_0}^2(n\pi)^2(k_v-2c_v\xi\Omega_n)+\\kL^2\left(\xi^2{\Omega_n}^2+{\Omega_d}^2\right)\end{pmatrix}\begin{pmatrix}\omega_n^4+2\omega_n^2\left(\xi^2{\Omega_n}^2-{\Omega_d}^2\right)\\+\left(\xi^2{\Omega_n}^2+{\Omega_d}^2\right)^2\end{pmatrix}\\
a_3&=\omega_n\Omega_d(-{v_0}^2(n\pi)^2+L^2\omega_n^2)\begin{pmatrix}{v_0}^2(n\pi)^2\left(2k_v\xi\Omega_n+c_v\left(\omega_n^2-\left(\xi^2{\Omega_n}^2+{\Omega_d}^2\right)\right)\right)+\\L^2\begin{pmatrix}2k_v\xi\Omega_n\left(\omega_n^2+2\xi^2{\Omega_n}^2-2{\Omega_d}^2\right)-\\c_v\left(\omega_n^2+3\xi^2{\Omega_n}^2-{\Omega_d}^2\right)\left(\xi^2{\Omega_n}^2+{\Omega_d}^2\right)\end{pmatrix}\end{pmatrix}\\
a_4&=e^{\xi\Omega_n t}\Omega_d\left((v_0 n\pi)^4+2L^2(v_0 n\pi)^2\left(\xi^2{\Omega_n}^2-{\Omega_d}^2\right)+L^4\left(\xi^2{\Omega_n}^2+{\Omega_d}^2\right)^2\right)\\
a_5&=\omega_n\left(-2k_v\xi\Omega_n+c_v\left(-\omega_n^2+\xi^2{\Omega_n}^2+{\Omega_d}^2\right)\right)\\
a_6&=\left(2c_v{\omega_n}^2\xi\Omega_n+k_v\left(-\omega_n^2+\xi^2{\Omega_n}^2+{\Omega_d}^2\right)\right)\\
a_7&=\omega_n((v_0 n\pi)^2-(L\omega_n)^2)\begin{pmatrix}-(k_v-c_v\xi\Omega_n)\left({\omega_n}^2+\xi^2{\Omega_n}^2\right)((v_0 n\pi)^2+(L\omega_n)^2)+\\\begin{pmatrix}(v_0 n\pi)^2(k_v+c_v\xi\Omega_n)\\+L^2\left(k_v{\omega_n}^2+c_v{\omega_n}^2\xi\Omega_n+6k_v\xi^2{\Omega_n}^2-2c_v\xi^3{\Omega_n}^3\right)\end{pmatrix}{\Omega_d}^2\\-L^2{\Omega_d}^4(k_v+3c_v\xi\Omega_n)\end{pmatrix}\\
a_8&=\begin{Bmatrix}\omega_n\Omega_d(\rho A)^2((\omega_n-\Omega_d)^2+(\xi\Omega_n)^2)((\omega_n+\Omega_d)^2+(\xi\Omega_n)^2)(-(v_0 n\pi)^2+(L\omega_n)^2)\\((v_0 n\pi-L\Omega_d)^2+(L\xi\Omega_n)^2)((v_0 n\pi+L\Omega_d)^2+(L\xi\Omega_n)^2)\end{Bmatrix}
\end{aligned}\quad(42)$$

After substituting the normalized normal mode into Eq. (33) and generalized coordinate Eq. (41) into Eq. (32), the response of the secondary nanobeam is determined, finally the response of the primary nanobeam is achieved by Eq. (13).

## 4. Results and discussion

For the sake of validation, our results are compared to a condition with no moving load and damping. Thus the free vibration of a double nanobeam with medium elastic layer is analyzed and the results are compared to *Murmo and Adhikar* paper. It worth nothing to mention that nanobeams vibrate in three different phases, out-phase, a fixed nanobeam and in-phase. It should be noted that the amount of $\overline{k}$ is equal to 1 and $\mu$ changes from 0 to 1. As it can be seen from Fig. 2, there is a good agreement between the results of this study and ref (Murmu and Adhikari 2010).

In this part, some numerical examples for a double nanobeam system that is under the moving load are presented. This nanobeam system consists of a viscoelastic medium layer which is modeled as a spring-damper system. For the sake of convenience, the following

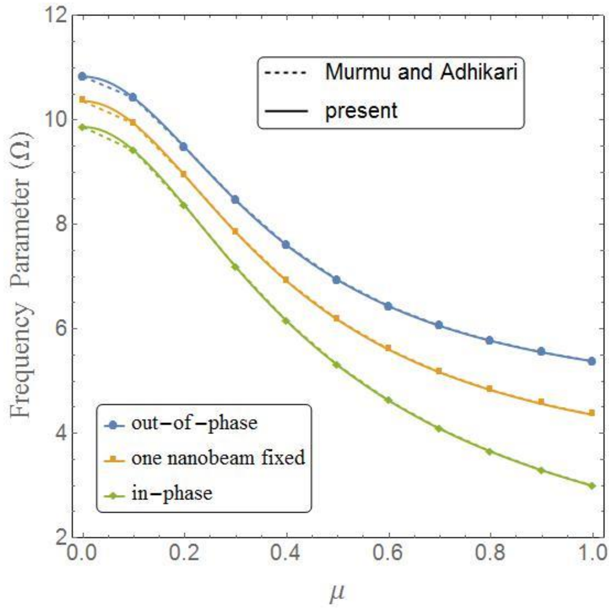


Fig. 2 Variation in the frequency parameter versus nonlocal parameter

nondimensionalization are used

$$\overline{W}_1 = \frac{w_1}{w_s},\quad \overline{W}_2 = \frac{w_2}{w_s},\quad \mu = \frac{e_0 a}{L},\quad \bar{\tau} = \frac{v_0 t}{L}, s = \frac{v_0}{v_{cr}} \text{ and } \bar{k} = \frac{k_v L^4}{EI} \tag{43}$$

$$\overline{W_1} = \frac{w_1}{w_s},\quad \overline{W_2} = \frac{w_2}{w_s},\quad \mu = \frac{e_0 a}{L},\quad \bar{\tau} = \frac{v_0 t}{L}, s = \frac{v_0}{v_{cr}} \text{ and } \bar{k} = \frac{k_v L^4}{EI}$$

Where $\overline{W}_1$ and $\overline{W}_2$ are the dimensionless deflection of the primary and secondary nanobeam in relation with $w_s$, respectively. $w_s$ represents the maximum static deflection of the nanobeam which is simply supported at $x = \frac{1}{2}$ and is equal to $w_s = \frac{P_0 L^3}{48EI}$. $\bar{k}$ denotes the dimensionless stiffness parameter and $s$represents the dimensionless velocity parameter which is nandimensinolizated in relation to $v_{cr}$. $v_{cr}$ is a critical velocity and is equal to $v_{cr} = \frac{\omega L}{\pi}$. $\mu$ and $\bar{\tau}$ indicates a dimensionless nonlocal parameter and dimensionless time, respectively. Prior to dealing with some numerical examples, it worth nothing to mention that the value of $\bar{\tau}$ is between 0 and 1 which means that where $\bar{\tau}$ is equal to 0, the $P_0$ load is at the start point and on the left side of the nanobeam and when $\bar{\tau}$ is equal to 1 the $P_0$ load is at the end point and on the right side of the nanobeam.

Fig. 3 shows the variation of dynamic deflection $\overline{W}_1$ for different values of $\xi = 0, 0.25, 0.5$ and $0.75$ with respect to the dimensionless time, different values of nonlocal parameter and the dimensionless stiffness. It should be mentioned that Fig. 2 (a1)-(a4) are related to $\bar{k} = 0.1$ and the nonlocal parameters which are equal $\mu = 0, 0.25, 0.5$ and $0.75$ respectively. Similarly, Fig. 3(b1)-(b4), 3(c1)-(c4) and 3(d1)-(d4) represent the nanobeam system with the dimensionless stiffness of 1, 10 and 100 respectively. It should be noted that when there is no damping ($\xi = 0$) and the dimensionless stiffness has low value, the weak elastic medium occurs and when the dimensionless parameter has high value the rigid coupling occurs. According to Fig. 3, it is clear

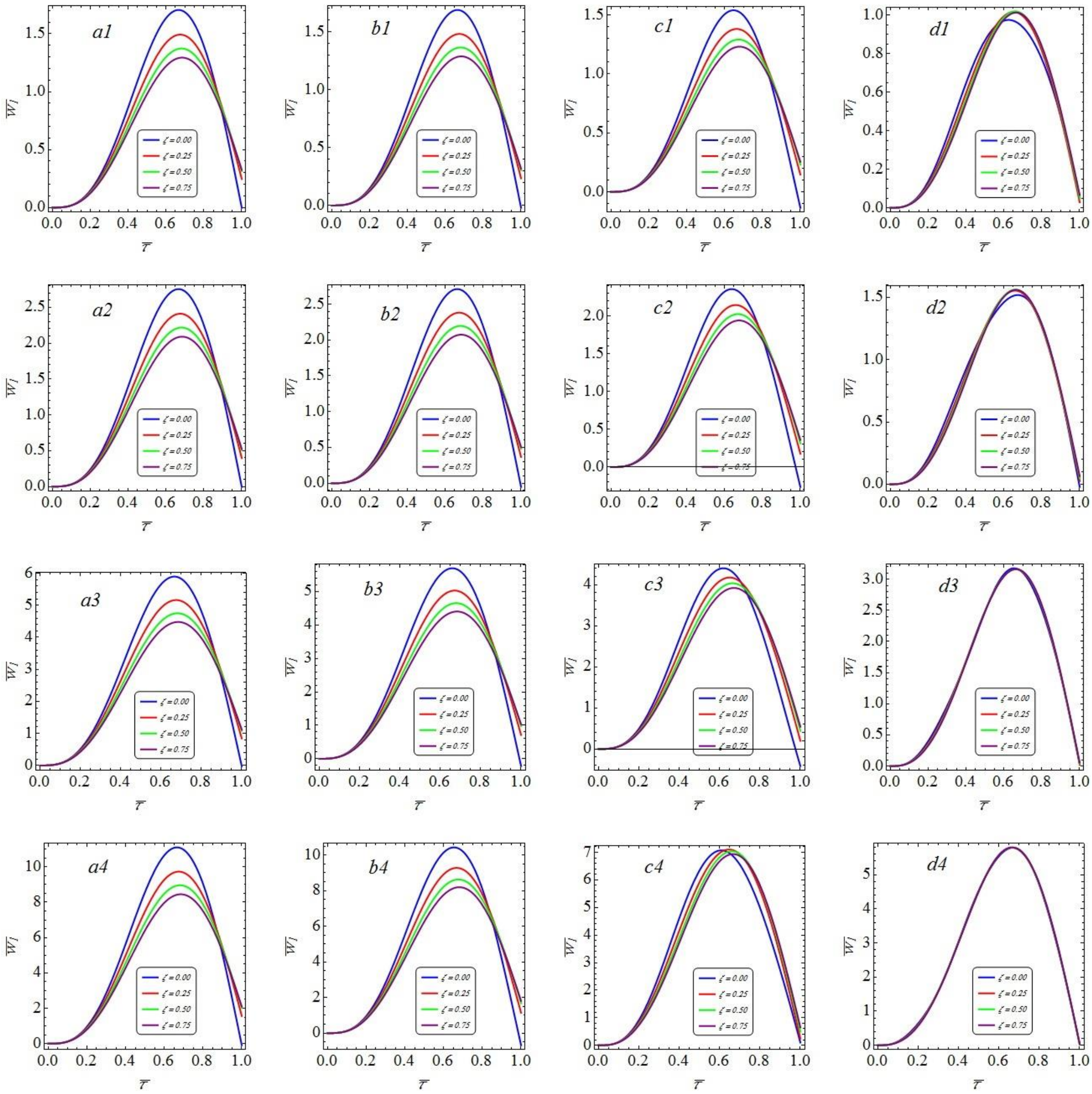


Fig. 3 The variation of dynamic deflection $\overline{W}_1$ for different values of $\xi = 0, 0.25, 0.5$ and 0.75 with respect to the dimensionless time, different values of nonlocal parameter and the dimensionless stiffness

that the maximum dynamic deflection of the primary nanobeam increases when the stiffness and nonlocal parameters decreases and increases, respectively. It should be said that the difference in the maximum dynamic deflections of the primary nanobeam that is with respect to different values of $\xi$ in a condition with low dimensionless stiffness is more than a condition with high dimensionless stiffness. In Fig. 3(d4) all the four values of $\xi$are coincident with each other. Also it can be seen from Fig. 3 that when the moving load has passed along 65% of the whole path of nanotube. the maximum of dynamic deflection occurs.

Fig. 4 shows the variation of dynamic deflection of the secondary nanobeam with respect to the dimensionless time and for different values of $\xi = 0, 0.25, 0.5$ and 0.75. As it is clear, Fig. 4(a1)-

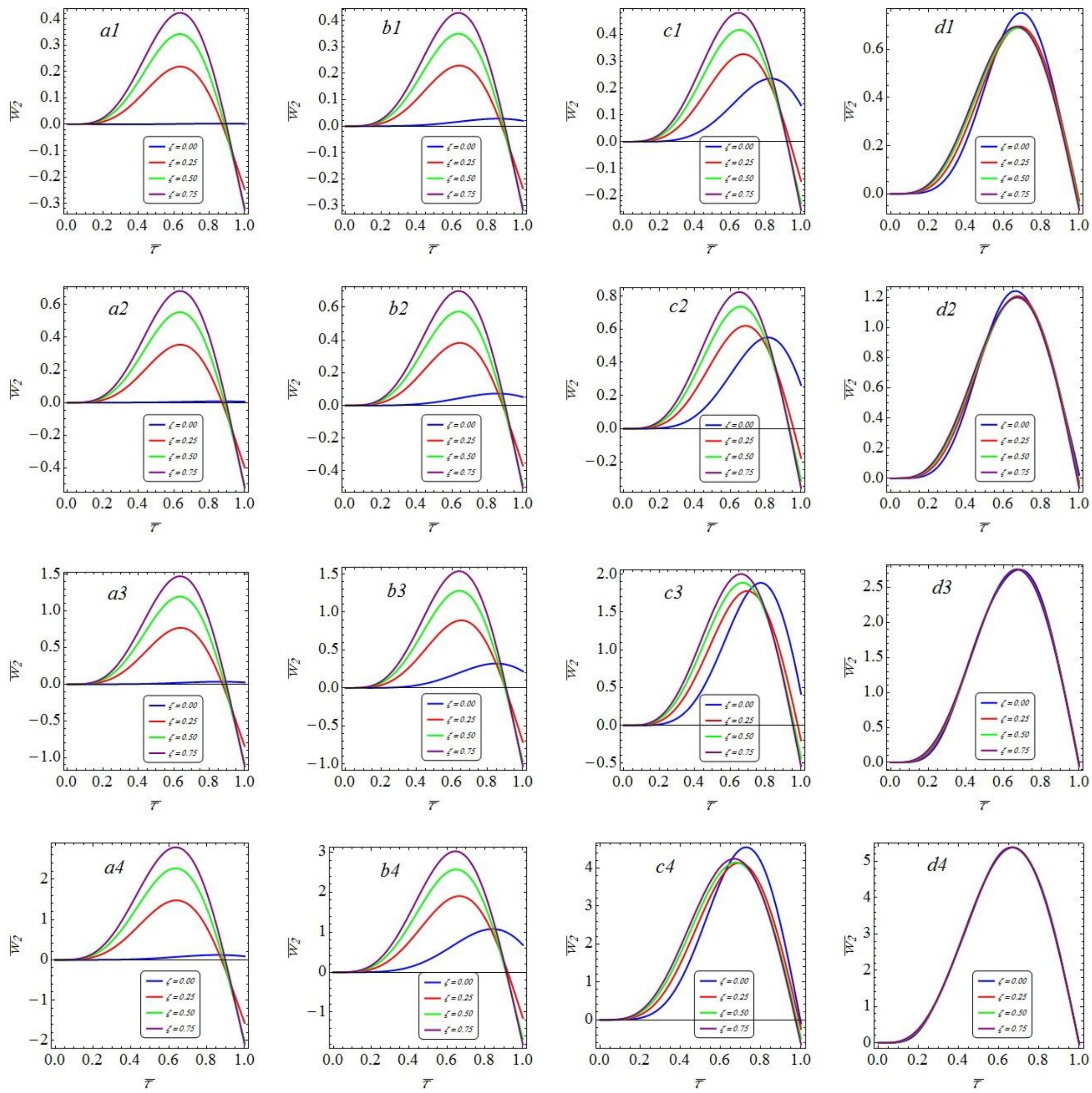

Fig. 4 The variation of dynamic deflection of the secondary nanobeam with respect to the dimensionless time and for different values of $\xi = 0, 0.25, 0.5$ and $0.75$

(a4) show the value of $W3$ for the dimensionless stiffness and nonlocal parameters of $\mu = 0, 0.25, 0.5$ and $0.75$ respectively. Fig. 4(b1)-(b4), (c1)-(c4) and (d1)-(d4) are illustrated for the nanobeam system with the dimensionless stiffness of 1, 10 and 100 respectively.

According to Figs. 4(a1)-(a4) it is clear that when $\xi$ is equal to zero and the dimensionless stiffness has low values ($\overline{k} = 0.1$) (weak coupling elastic condition), the dynamic deflection of the secondary nanobeam is zero. In this condition, as $\xi$ increases, the maximum dynamic deflection increases.

According to Fig. 3, increasing in dimensionless stiffness and nonlocal parameter, tends to increase of the maximum dynamic deflection Clearly, by increasing the dimensionless stiffness,

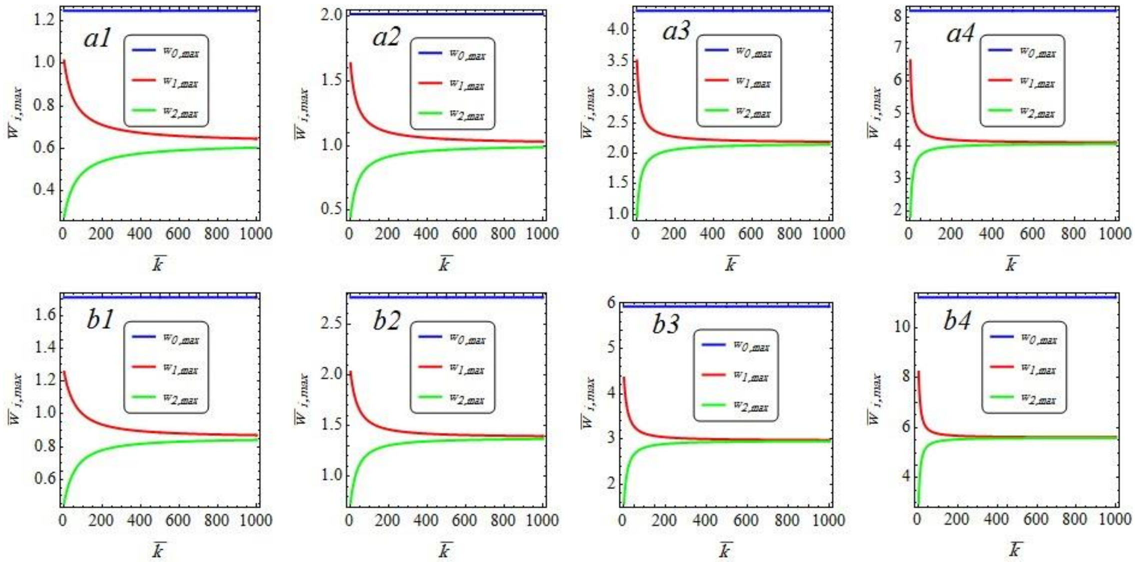

Fig. 5 The variation of the maximum dynamic deflection $\overline{W}_{i,\max}$ in terms of the dimensionless stiffness parameter $\bar{k}$

the difference between the maximum dynamic deflection with respect to different values of $\xi$, decreases, same as Fig. 3.

In this section, the variation of the maximum dynamic deflection in terms of different parameters is analyzed. It should be mentioned that, the maximum dynamic deflection is represented by $\overline{W}_{i,\max}$, $i = 0,1,2$ and $\overline{W}_{0,\max}$, $\overline{W}_{1,\max}$ and $\overline{W}_{2,\max}$ indicate the relative maximum dynamic deflection of the primary and the secondary nanobeam, the maximum dynamic deflection of the primary nanobeam and the maximum dynamic deflection of the secondary nanobeam, respectively.

Fig. 5 shows the variation of the maximum dynamic deflection $\overline{W}_{i,\max}$ in terms of the dimensionless stiffness parameter $\bar{k}$ which changes from 0 to 1000. Fig. 5(a1)-(a4) indicate the dimensionless velocity $s = 0.25$ in terms of the nonlocal parameters $\mu = 0, 0.25, 0.5$ and $0.75$, respectively and similarly Fig. 5(b1)-(b4) show the dimensionless velocity $s = 0.75$ in terms of $\mu = 0, 0.25, 0.5$ and $0.75$ respectively. As it is clear, the maximum dynamic deflection does not change as the dimensionless stiffness increases. This reason was described in Eq. (29) which is independent of stiffness. Also as $\bar{k}$ increases, $\overline{W}_{1,\max}$ and $\overline{W}_{2,\max}$ decreases and increases, respectively and their diagrams are symmetric. Clearly, as $\bar{k}$ increases, $\overline{W}_{1,\max}$ and $\overline{W}_{2,\max}$ are converged to each other and as the nonlocal parameter and dimensionless velocity increases their convergence rate increases.

The variation of $\overline{W}_{i,\max}$ with respect to the nonlocal parameter that changes from 0 to 1, is illustrated in Fig. 6. $\overline{W}_{i,\max}$ for $s = 0.25$ and $\bar{k} = 1, 10$ and $100$ are depicted in Fig. 6(a1)-(a3), respectively. Similarly, $\overline{W}_{i,\max}$ for $s = 0.75$ and $\bar{k} = 1, 10$ and $100$ are illustrated in Fig. 6(b1)-(b3), respectively. It can be seen that, increasing in the nonlocal parameters, tends to increase $\overline{W}_{0,\max}$, $\overline{W}_{1,\max}$ and $\overline{W}_{2,\max}$.

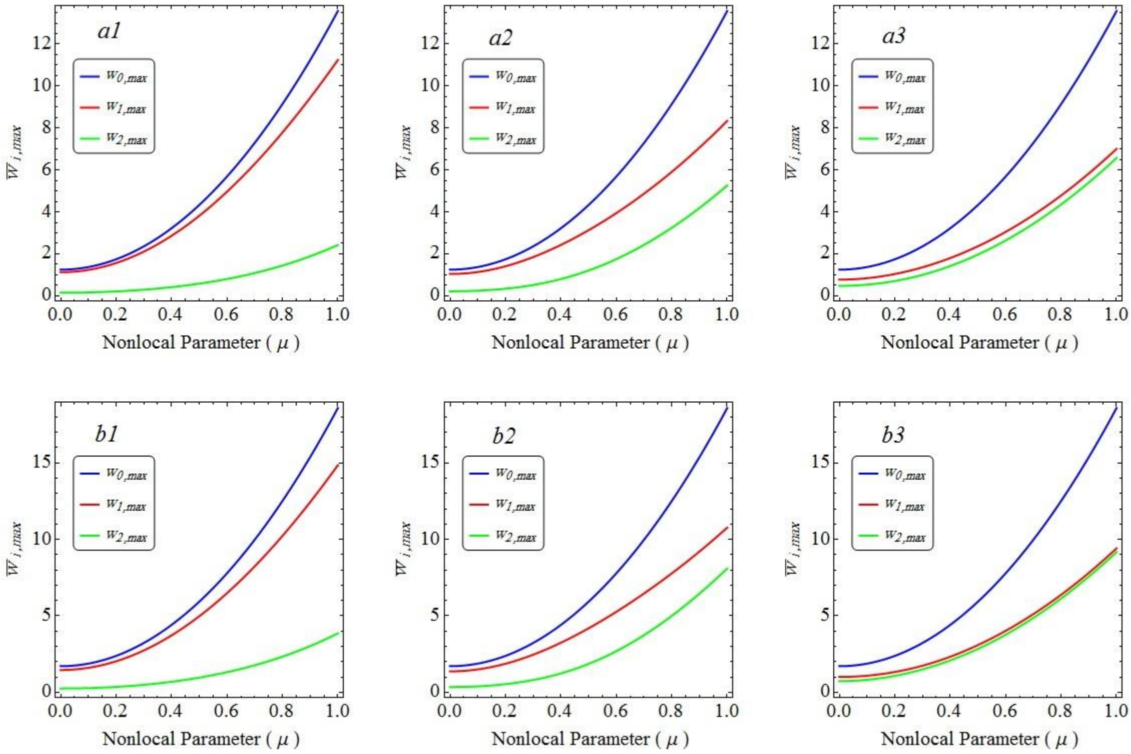


Fig. 6 The variation of $\overline{W}_{i,\max}$ with respect to the nonlocal parameter

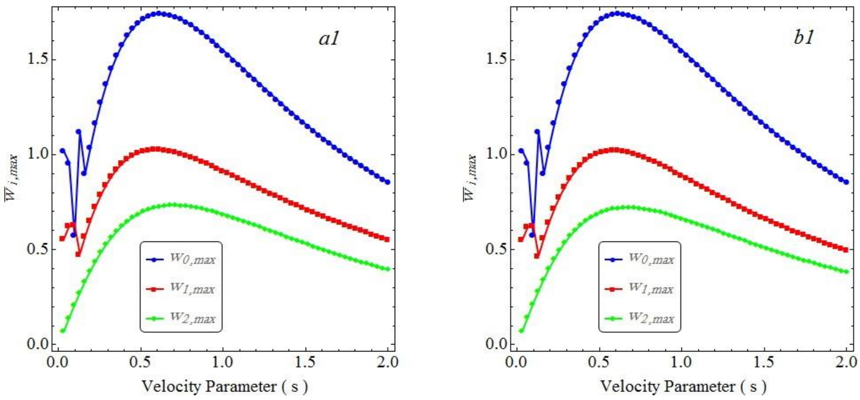


Fig. 7 The variation of $\overline{W}_{i,\max}$ with respect to dimensionless velocity

Fig. 7 shows the variation of $\overline{W}_{i,\max}$ with respect to dimensionless velocity that changes from 0 to 2. The maximum dynamic deflection for $\xi = 0.25$ and nonlocal parameter $\mu$=0, 0.25, 0.5 and 0.75 is depicted in Fig. 7(a1)-(a4), respectively. Similarly, the maximum dynamic deflection for $\xi = 0.75$ and nonlocal parameter 0, 0.25 and 0.75 is illustrated in Fig. 6(b1)-(b4), respectively.

As it is clear, as the dimensionless velocity increases, firstly the $\overline{W}_{i,\max}$ increases and then when $0.5 < s < 0.65$ decreases. As the nonlocal parameter increases, $\overline{W}_{1,\max}$ and $\overline{W}_{2,\max}$ are

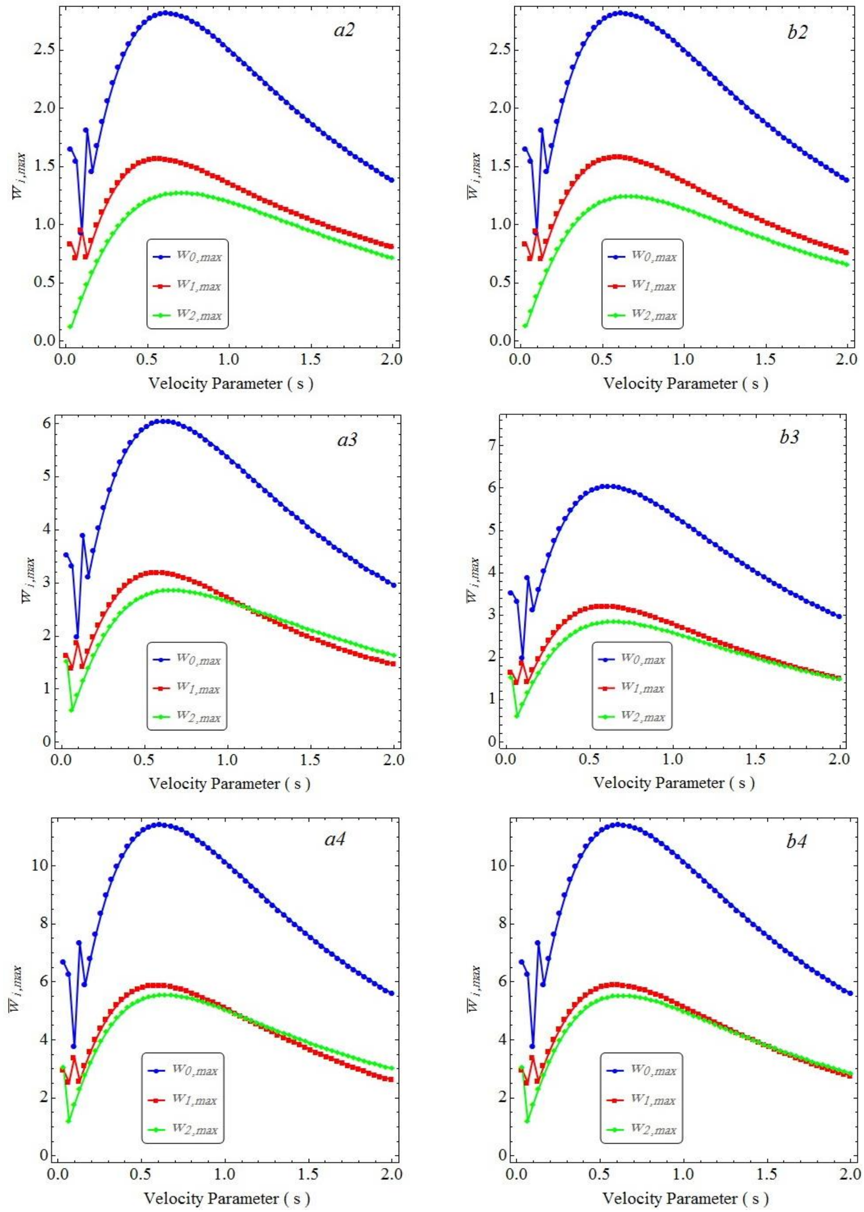


Fig. 7 Continued

converged to each other.

The variation of $\overline{W}_{i,\max}$ in terms of the damping ratio $\xi$ is shown in Fig. 8. Clearly, the diagram of $\overline{W}_{0,\max}$ is a straight line which denotes that it is not dependent on $\xi$.

It is clear that as the damping ratio increases, the $\overline{W}_{1,\max}$ increases and is converged to $\overline{W}_{0,\max}$ and symmetrically the $\overline{W}_{2,\max}$ decreases and is converged to zero. Also it can be concluded that, by increasing the dimensionless stiffness in the initial values of $\xi$, $\overline{W}_{1,\max}$ and $\overline{W}_{2,\max}$ come closer

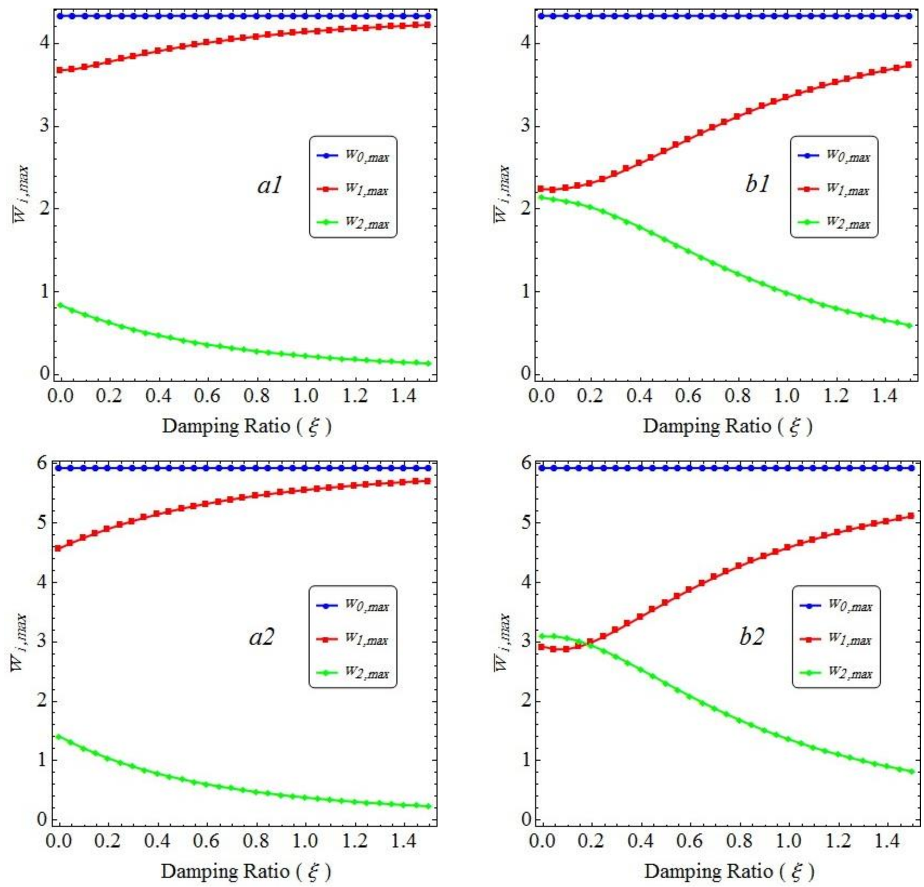


Fig. 8 The variation of $\overline{W}_{i,\max}$ in terms of the damping ratio $\xi$

to each other but as $\xi$ increases they are diverged from each other.

## 5. Conclusions

A dynamic behavior of a double nanobeam system, with a medium viscoelastic layer, under a moving load, using an Eringen nonlocal theory, was analyzed in this paper. The nonlocal equations were based on the Euler–Bernoulli model, the simply supported boundary condition was considered, and the viscoelastic medium layer was modeled which was based on a spring-damper system. An exact solution was resulted for the primary and secondary nanobeams. By nondimensionalization of the parameters, a wide range of examples and diagrams were achieved which made the nonlocal parameters, the velocity of the moving load, the stiffness parameter and the damping ratio to be accurately analyzed. It was determined that

- As the nonlocal parameter increases, the maximum dynamic deflection increases, which the importance of the nonclassic theories.
- By increasing the stiffness parameter, the maximum dynamic deflection and damping ratio of the primary nanobeam decreases and increases respectively.

• by increasing the dimensionless stiffness in the initial values of $\xi$, $\overline{W}_{1,\max}$ and $\overline{W}_{2,\max}$ come closer to each other but as $\xi$ increases they are diverged from each other.
• Increasing in the stiffness parameters of the secondary nanobeam, results in increasing and decreasing of its maximum dynamic deflection and damping ratio, respectively.
• When the value of dimensionless velocity is between 0.5 to 0.75, the maximum dynamic deflection occurs

## References


Al-Huniti, N.S. and Alahmad, S.T. (2017), "Transient thermo-mechanical response of a functionally graded beam under the effect of a moving heat source", *Adv. Mater. Res.*, **6**(1), 27. https://doi.org/10.12989/amr.2017.6.1.027.

Bastanfar, M., Hosseini, S.A., Sourki, R. and Khosravi, F. (2019), "Flexoelectric and surface effects on a cracked piezoelectric nanobeam: Analytical resonant frequency response", *Arch. Mech. Eng.*, **66**(4), 417-437. https://doi.org/10.24425/ame.2019.131355.

Bensaid, I., Cheikh, A., Mangouchi, A. and Kerboua, B. (2017), "Static deflection and dynamic behavior of higher-order hyperbolic shear deformable compositionally graded beams", *Adv. Mater. Res.*, **6**(1), 13. https://doi.org/10.12989/amr.2017.6.1.013.

Dai, H., Hafner, J.H., Rinzler, A.G., Colbert, D.T. and Smalley, R.E. (1996), "Nanotubes as nanoprobes in scanning probe microscopy", *Nature*, **384**(6605), 147-150. https://doi.org/10.1038/384147a0.

Ebrahimi, F. and Barati, M.R. (2017), "Thermal-induced nonlocal vibration characteristics of heterogeneous beams", *Adv. Mater. Res.*, **6**(2), 93. https://doi.org/10.12989/amr.2017.6.2.093.

Ebrahimi, F., Mahmoodi, F. and Barati, M.R. (2017), "Thermo-mechanical vibration analysis of functionally graded micro/nanoscale beams with porosities based on modified couple stress theory", *Adv. Mater. Res.*, **6**(3), 279. https://doi.org/10.12989/amr.2017.6.3.279.

Eichenfield, M., Chan, J., Camacho, R.M., Vahala, K.J. and Painter, O. (2009), "Optomechanical crystals", *Nature*, **462**(7269), 78-82. https://doi.org/10.1038/nature08524.

Eringen, A.C. (1972), "Nonlocal polar elastic continua", *Int. J. Eng. Sci.*, **10**(1), 1-16. https://doi.org/10.1016/0020-7225(72)90070-5.

Fernández-Sáez, J. and Zaera, R. (2017), "Vibrations of Bernoulli-Euler beams using the two-phase nonlocal elasticity theory", *Int. J. Eng. Sci.*, **119**, 232-248. https://doi.org/10.1016/j.ijengsci.2017.06.021.

Frank, I.W., Deotare, P.B., McCutcheon, M.W. and Lončar, M. (2010), "Programmable photonic crystal nanobeam cavities", *Opt. Expr.*, **18**(8), 8705-8712. https://doi.org/10.1364/OE.18.008705.

Hamidi, B.A., Hosseini, S.A., Hassannejad, R. and Khosravi, F. (2019), "An exact solution on gold microbeam with thermoelastic damping via generalized Green-Naghdi and modified couple stress theories", *J. Therm. Stress.*, **43**(2), 157-174. https://doi.org/10.1080/01495739.2019.1666694.

Hamidi, B.A., Hosseini, S.A., Hassannejad, R. and Khosravi, F. (2020), "Theoretical analysis of thermoelastic damping of silver nanobeam resonators based on Green–Naghdi via nonlocal elasticity with surface energy effects", *Eur. Phys. J. Plus*, **135**(1), 35. https://doi.org/10.1140/epjp/s13360-019-00037-8.

Hayati, H., Hosseini, S.A. and Rahmani, O. (2016), "Coupled twist–bending static and dynamic behavior of a curved single-walled carbon nanotube based on nonlocal theory", *Microsyst. Technol.*, **23**, 2393-2401. https://doi.org/10.1007/s00542-016-2933-0.

Hosseini, S. and Rahmani, O. (2016), "Surface effects on buckling of double nanobeam system based on nonlocal Timoshenko model", *Int. J. Struct. Stab. Dyn.*, **16**(10), 1550077. https://doi.org/10.1142/S0219455415500777.

Hosseini, S.A. and Khosravi, F. (2020), "Exact solution for dynamic response of size dependent torsional vibration of CNT subjected to linear and harmonic loadings", *Adv. Nano Res.*, **8**(1), 25. https://doi.org/10.12989/anr.2020.8.1.025.

Hosseini, S.A., Khosravi, F. and Ghadiri, M. (2019), "Moving axial load on dynamic response of single-walled carbon nanotubes using classical, Rayleigh and Bishop rod models based on Eringen's theory", *J. Vib. Control*, **26**(11-12), 913-928. https://doi.org/10.1177/1077546319890170.

Hosseini, S.A., Khosravi, F. and Ghadiri, M. (2020), "Effect of external moving torque on dynamic stability of carbon nanotube", *J. Nano Res.*, **61**, 118-135. https://doi.org/10.4028/www.scientific.net/JNanoR.61.118.

Hosseini, S.A.H. and Rahmani, O. (2016), "Free vibration of shallow and deep curved FG nanobeam via nonlocal Timoshenko curved beam model", *Appl. Phys. A*, **122**(3), 1-11. https://doi.org/10.1007/s00339-016-9696-4.

Khaniki, H.B. (2018), "Vibration analysis of rotating nanobeam systems using Eringen's two-phase local/nonlocal model", *Physica E: Low Dimens. Syst. Nanostr.*, **99**, 310-319. https://doi.org/10.1016/j.physe.2018.02.008.

Khosravi, F., Hosseini, S.A. and Hamidi, B.A. (2020), "On torsional vibrations of triangular nanowire", *Thin Wall. Struct.*, **148**, 106591. https://doi.org/10.1016/j.tws.2019.106591.

Khosravi, F., Hosseini, S.A. and Norouzi, H. (2020), "Exponential and harmonic forced torsional vibration of single-walled carbon nanotube in an elastic medium", *Proc. Inst. Mech. Eng., Part C: J. Mech. Eng. Sci.*, **234**(10), 1928-1942. https://doi.org/10.1177/0954406220903341.

Khosravi, F., Hosseini, S.A. and Tounsi, A. (2020), "Torsional dynamic response of viscoelastic SWCNT subjected to linear and harmonic torques with general boundary conditions via Eringen's nonlocal differential model", *Eur. Phys. J. Plus*, **135**(2), 183. https://doi.org/10.1140/epjp/s13360-020-00207-z.

Kim, P. and Lieber, C.M. (1999), "Nanotube nanotweezers", *Sci.*, **286**(5447), 2148-2150. https://doi.org/10.1126/science.286.5447.2148.

Kunbar, L.A.H., Alkadhimi, B.M., Radhi, H.S. and Faleh, N.M. (2020), "Flexoelectric effects on dynamic response characteristics of nonlocal piezoelectric material beam", *Adv. Mater. Res.*, **8**(4), 259. https://doi.org/10.12989/amr.2019.8.4.259.

Liew, K.M., He, X.Q. and Kitipornchai, S. (2006), "Predicting nanovibration of multi-layered graphene sheets embedded in an elastic matrix", *Acta Materialia*, **54**(16), 4229-4236. https://doi.org/10.1016/j.actamat.2006.05.016.

Murmu, T. and Adhikari, S. (2010), "Nonlocal transverse vibration of double-nanobeam-systems", *J. Appl. Phys.*, **108**(8), 083514. https://doi.org/10.1063/1.3496627.

Murmu, T. and Adhikari, S. (2011), "Nonlocal vibration of bonded double-nanoplate-systems", *Compos. Part B: Eng.*, **42**(7), 1901-1911. https://doi.org/10.1016/j.compositesb.2011.06.009.

Murmu, T. and Adhikari, S. (2012), "Nonlocal elasticity based vibration of initially pre-stressed coupled nanobeam systems", *Eur. J. Mech.-A/Solid.*, **34**, 52-62. https://doi.org/10.1016/j.euromechsol.2011.11.010.

Pirmohammadi, A.A., Pourseifi, M., Rahmani, O. and Hoseini, S.A.H. (2014), "Modeling and active vibration suppression of a single-walled carbon nanotube subjected to a moving harmonic load based on a nonlocal elasticity theory", *Appl. Phys. A*, **117**(3), 1547-1555. https://doi.org/10.1007/s00339-014-8592-z.

Pouresmaeeli, S., Fazelzadeh, S.A. and Ghavanloo, E. (2012), "Exact solution for nonlocal vibration of double-orthotropic nanoplates embedded in elastic medium", *Compos. Part B: Eng.*, **43**(8), 3384-3390. https://doi.org/10.1016/j.compositesb.2012.01.046.

Pourseifi, M., Rahmani, O. and Hoseini, S.A.H. (2015), "Active vibration control of nanotube structures under a moving nanoparticle based on the nonlocal continuum theories", *Meccanica*, **50**(5), 1351-1369. https://doi.org/10.1007/s11012-014-0096-6.

Radić, N., Jeremić, D., Trifković, S. and Milutinović, M. (2014), "Buckling analysis of double-orthotropic nanoplates embedded in Pasternak elastic medium using nonlocal elasticity theory", *Compos. Part B: Eng.*, **61**, 162-171. https://doi.org/10.1016/j.compositesb.2014.01.042.

Rahmani, O., Asemani, S.S. and Hosseini, S.A.H. (2015), "Study the buckling of functionally graded nanobeams in elastic medium with surface effects based on a nonlocal theory", *J. Comput. Theor. Nanosci.*, **12**(10), 3162-3170. https://doi.org/10.1166/jctn.2015.4095.

Rahmani, O., Hosseini, S.A.H. and Hayati, H. (2016), "Frequency analysis of curved nano-sandwich structure based on a nonlocal model", *Modern Phys. Lett. B*, **30**(10), 1650136.

https://doi.org/10.1142/S0217984916501360.

Rahmani, O., Hosseini, S.A.H., Noroozi Moghaddam, M.H. and Fakhari Golpayegani, I. (2015), "Torsional vibration of cracked nanobeam based on nonlocal stress theory with various boundary conditions: An analytical study", *Int. J. Appl. Mech*., **07**(03), 1550036. https://doi.org/10.1142/S1758825115500362.

Rahmani, O. and Pedram, O. (2014), "Analysis and modeling the size effect on vibration of functionally graded nanobeams based on nonlocal Timoshenko beam theory", *Int. J. Eng. Sci*., **77**, 55-70. https://doi.org/10.1016/j.ijengsci.2013.12.003.

Romano, G., Barretta, R., Diaco, M. and Marotti de Sciarra, F. (2017), "Constitutive boundary conditions and paradoxes in nonlocal elastic nanobeams", *Int. J. Mech. Sci*., **121**, 151-156. https://doi.org/10.1016/j.ijmecsci.2016.10.036.

Wang, Y.B., Zhu, X.W. and Dai, H.H. (2016), "Exact solutions for the static bending of Euler-Bernoulli beams using Eringen's two-phase local/nonlocal model", *AIP Adv*., **6**(8), 085114. https://doi.org/10.1063/1.4961695.

Zhang, P. and Qing, H. (2021), "Closed-form solution in bi-Helmholtz kernel based two-phase nonlocal integral models for functionally graded Timoshenko beams", *Compos. Struct*., **265**, 113770. https://doi.org/10.1016/j.compstruct.2021.113770.

Zhang, P. and Qing, H. (2022), "Free vibration analysis of Euler–Bernoulli curved beams using two-phase nonlocal integral models", *J. Vib. Control*, **28**(19-20), 2861-2878. https://doi.org/10.1177/10775463211022483.

Zhang, P. and Qing, H. (2022), "Well-posed two-phase nonlocal integral models for free vibration of nanobeams in context with higher-order refined shear deformation theory", *J. Vib. Control*, **28**(23-24), 3808-3822. https://doi.org/10.1177/10775463211039902.

Zhang, P., Schiavone, P. and Qing, H. (2022), "Local/nonlocal mixture integral models with bi-Helmholtz kernel for free vibration of Euler-Bernoulli beams under thermal effect", *J. Sound Vib*., **525**, 116798. https://doi.org/10.1016/j.jsv.2022.116798.

*CC*